Electrochemical and Solid-State Letters, **13** (11) P15-P17 (2010)
1099-0062/2010/13(11)/P15/3/$28.00 © The Electrochemical Society

High Seebeck Coefficient BiSbTe Nanowires

Raja S. Mannam[z] **and Despina Davis**[*,z]

Institute for Micromanufacturing, Louisiana Tech University, Ruston, Louisiana 71270, USA

Bismuth antimony telluride (BiSbTe) nanowires were electrodeposited at constant potentials into polycarbonate templates from a tartaric–nitric acid electrolyte. Optimum deposition potentials were obtained from polarization and compositional analysis. X-ray diffraction analysis showed a preferential (015) orientation for the nanowires. The $Bi_2Sb_{0.6}Te_3$ nanowire sample deposited at −150 mV showed a high Seebeck coefficient (S) of −630 μV/K.
 [DOI: 10.1149/1.3481712]

Manuscript submitted June 2, 2010; revised manuscript received July 29, 2010. Published September 9, 2010.

Concerns over the depleting fossil fuels and increasing global warming threat stimulated the researchers to develop efficient thermoelectric materials, defined by the figure of merit as $ZT = S^2\sigma T/k$, where S is the Seebeck coefficient, σ is electrical conductivity, T is the absolute temperature, and k is thermal conductivity.[1] The ZT of the current bulk materials is limited to 1;[2] however, a value higher than 3 is required to compete with conventional energy techniques. Increasing the thermoelectric power factor ($S^2\sigma$) and decreasing the thermal conductivity are the two main approaches to increase ZT. In superlattice Bi_2Te_3/Sb_2Te_3 thin films, a high ZT of 2.4 was obtained mainly by the decreased lattice thermal conductivity.[3] Taking into account the improved density of states resulting in higher power factors and decreased phonon thermal conductivity due to surface scattering, Dresselhaus's group[2,4] predicted an even higher ZT for one-dimensional nanostructures. Also, experimental results showed[5] that BiTe nanowires have lower thermal conductivity than their bulk counterparts.

Stacy's group[6] was the first to report electrodeposition of BiSbTe nanowires in porous alumina templates using a tartaric–nitric acid based electrolyte and proposed different mechanisms for the reduction of BiSbTe alloys following the overall reaction

$$3HTeO_2 + 2(1 - x)Bi^{3+} + 2xSbO^+ + (9 + 4x)H^+ + 18e^- \rightarrow (Bi_{1-x}Sb_x)_2Te_3 + (6 + 2x)H_2O$$

Del Frari et al.[7,8] studied the optimum conditions for electrodeposition of $Bi_{0.5}Sb_{1.5}Te_3$ alloys from a tartaric–perchloric acid bath and measured a thin-film power factor of 600 μWK^{-2} m^{-1}. Xiao et al.[9] electrodeposited $(Bi_{0.3}Sb_{0.7})_2Te_3$ and $Bi_{1.8}Sb_{0.1}Te_{3.1}$ nanowires in polycarbonate template and described their semiconducting nature from the temperature-dependent current–voltage plots. Although few articles are available on the electrodeposition of BiSbTe nanowires,[6-9] there is a need for their thermoelectric characterization. Our current research focuses on achieving higher Seebeck coefficients, by optimizing the alloy composition, using electrodeposited of BiSbTe nanostructures. To the best of our knowledge, the reported Seebeck coefficients here are the highest values among the electrodeposited BiTe alloy family (BiSbTe and BiSeTe) materials.[10-12]

Experimental

BiSbTe nanowires were electrodeposited into polycarbonate membranes using a Solartron 1287 function generator at constant potentials and room temperature from a tartaric–nitric acid based electrolyte. Being difficult to dissolve, Sb_2O_3 was treated with tartaric acid as a complexing agent to increase its solubility in water, and the obtained solution was mixed with a separately prepared Bi_2O_3 and TeO_2 electrolyte dissolved in HNO_3, followed by the addition of deionized (DI) water to make the final composition of 2.5 mM Bi^{3+}, 5 mM SbO^+, 10 mM TeO_2, 0.2 M tartaric acid, and 1 M HNO_3. For the polarization analysis, the individual Bi^{3+} and $HTeO_2^+$ electrolytes were obtained by dissolving them in 1 M HNO_3, while SbO^+ electrolyte was prepared using 0.2 M tartaric acid and 1 M HNO_3. The reference and counter electrodes were saturated calomel electrode (SCE) and a platinum (99.99%) mesh connected to a platinum wire, respectively. A 60 nm thick Au layer was sputtered on commercially available 50 nm pore size polycarbonate (Whatman) templates to deposit the nanostructures. Polycarbonate membranes (6 μm thickness, 6×10^8 pores/cm^2) had lower thermal conductivity compared to alumina membranes which made them ideal for nanowire-based thermoelectric devices. The obtained electrodeposited nanostructures embedded in the template were separated by dissolving the polycarbonate using dichloromethane (Alfa Aesar) followed by rinsing with DI water several times before imaging them with a scanning electron microscope (SEM, Hitachi S4800). Qualitative and quantitative composition analysis was obtained using an energy-dispersive spectroscope (Hitachi 4800). The crystal structure of the nanowires was studied using an X-ray diffractometer (Bruker D8 Discover, Cu Kα radiation). The micromanipulator 916776 electrical probe station with a tip contacting diameter of 10 μm was used to make precise contacts on the samples for electrical measurements.[13] A Cu strip was used as a reference for voltage measurements, while an Omega K-type thermocouple was used to measure temperature. The measuring setup was verified by measuring Seebeck coefficients of pure Bi nanowires and comparing with the data available in literature. A room-temperature (300 K) Seebeck coefficient of −106 μV/K was measured for 50 nm Bi nanowires. To compare with the literature (Fig. 5), room-temperature Seebeck coefficients of −80 μV/K were obtained for 150 nm Bi wires,[14] while a value of approximately −102 μV/K was measured for single crystal Bi.[15] Details about the measurement setup were discussed previously.[13]

Results and Discussion

Figure 1 shows the polarization curves of the individual Bi^{3+}, $HTeO_2^+$, SbO^+, and their combined electrolyte. The goal of this analysis is to identify suitable deposition potentials to obtain BiSbTe alloys with different compositions. In the individual electrolytes, Bi^{3+} and $HTeO_2^+$ limiting currents were reached at −115 and −90 mV, respectively, while SbO^+ has two minor limiting currents at −170 and −225 mV and a major limiting current at −280 mV. This is consistent with the earlier articles[7] showing higher reduction potentials for SbO^+. The polarization plot of the combined electrolyte can be divided into three reduction regions R_1 (0 to −70 mV), R_2 (−70 to −180 mV), and R_3 (>−180 mV). For the lower deposit potentials in the region R_1 the alloy current has a major contribution from the more noble elements Bi^{3+} and $HTeO_2^+$, which is justified by the composition analysis shown in Fig. 2; therefore, stoichiometric Bi_2Te_3 alloy nanowires were then obtained at −20 mV. A two-step reduction process, with the initial reduction of $HTeO_2^+$ to Te, followed by the further reduction of Te to the more stable Bi_2Te_3 characterizes this electrodeposition window.[7,16]

The reduction of all three elements was observed in the region R_2 forming different BiSbTe alloy combinations. Indicating the individual Bi^{3+} and $HTeO_2^+$ components, two limiting currents were ob-

* Electrochemical Society Active Member.
[z] E-mail: rsm020@latech.edu; ddavis@latech.edu

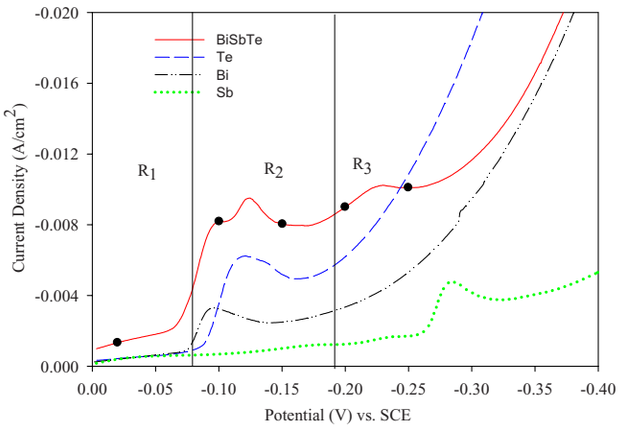

Figure 1. (Color online) Polarization plot of Bi^{3+}, $HTeO_2^+$, SbO^+, and the combined BiSbTe solution.

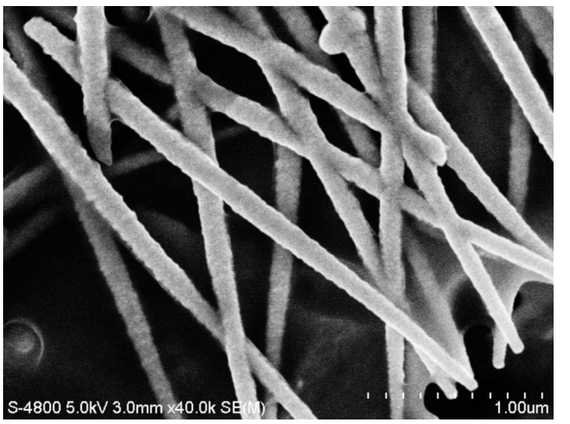

Figure 3. SEM image of the nanowires deposited in polycarbonate membranes.

served at −100 and −125 mV; however, the negative shift in the reduction potentials in the combined electrolyte, compared to the individual components, contradicts the positive shift observed in the BiTe electrolytes.[13,16] This behavior can be attributed to the formation of antimony–tartaric acid complex cations, which tend to shift the reduction potentials to more negative values.[6] The concentration of antimony in the deposited alloy remained relatively constant for depositions in the R_2 region, obtaining stoichiometric $Bi_{1.7}Sb_{0.58}Te_3$ and $Bi_2Sb_{0.6}Te_3$ at −100 and −150 mV, respectively. An overall third limiting current was observed in the R_3 region, while the composition analysis of the nanowires sample deposited at −200 and −250 mV shows a further increase in the antimony composition. In the R_3 region, reduction starts with the formation of H_2Te from $HTeO_2^+$, followed by the electrochemical reaction of H_2Te with Bi^{3+} and SbO^+, to form BiSbTe alloys.[6]

Figure 3 shows the X-ray diffraction (XRD) analysis of the nanowires deposited in polycarbonate membranes at various potentials −20, −150, and −150 mV. Te-rich nanowires deposited at lower potentials have a preferential (015) orientation, while the Sb rich nanowires have the preferential (110) orientation. Figure 4 shows the corresponding SEM image of the nanowires deposited at −150 mV. Even though the specified pore diameter was 50 nm, the deposited nanowires show an increasing pore diameter along their longitudinal axis and an average diameter of 110 nm was measured for obtained nanowires. Fully grown nanowires having different alloy compositions, deposited at −20, −100, −150, −200, and −250 mV (Fig. 1 bullets), were chosen for thermoelectric characterization.

Figure 5 shows the Seebeck coefficients of BiSbTe nanowires. All the measured samples showed a decreasing trend in Seebeck coefficients with temperature and the negative values indicate their n-type behavior. The highest Seebeck coefficient of −630 μV/K was obtained at 300 K for the nanowire sample electrodeposited at a potential of −150 mV. The antimony content in the BiSb alloys has a major influence on the nanowire diameter at which a semimetal to semiconductor transition can be observed, which is due to the increased distance between the electron and hole sub-bands. Compared to the pure bismuth nanowires (<50 nm), addition of antimony increases the diameter at which this transition could be observed, indicating that even the larger diameter BiSb alloy wires, with an optimum antimony composition, can exhibit a semiconducting behavior resulting in higher Seebeck coefficients.[17,18] The same phenomenon can be attributed to the high Seebeck coefficients achieved in $Bi_2Sb_{0.6}Te_{2.9}$ nanowires, which have the 11% antimony and a diameter of 110 nm. These values are close to the optimum antimony percentage and wire diameter predicted to for BiSb nanowires.[4] Antimony rich (20–23%) nanowires deposited at potentials −200 and −250 mV exhibited lower Seebeck coefficients of −244 and −325 μV/K at 375 K, respectively, noting that even the lowest Seebeck coefficients are higher than their bulk

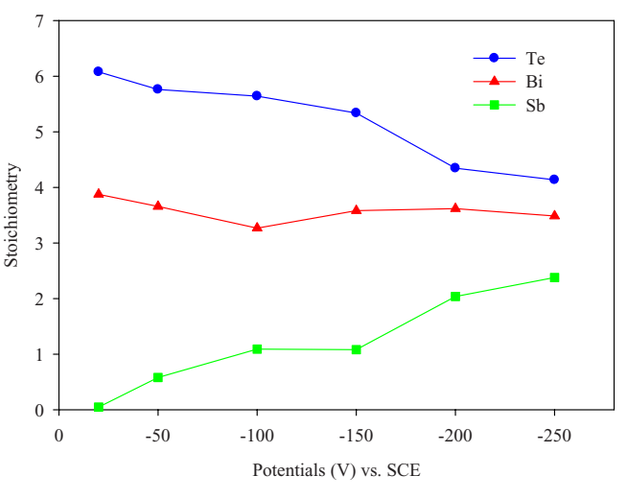

Figure 2. (Color online) Plot showing the stoichiometric Bi, Te, and Sb ratios in the deposited alloy with respect to the deposition potential vs SCE.

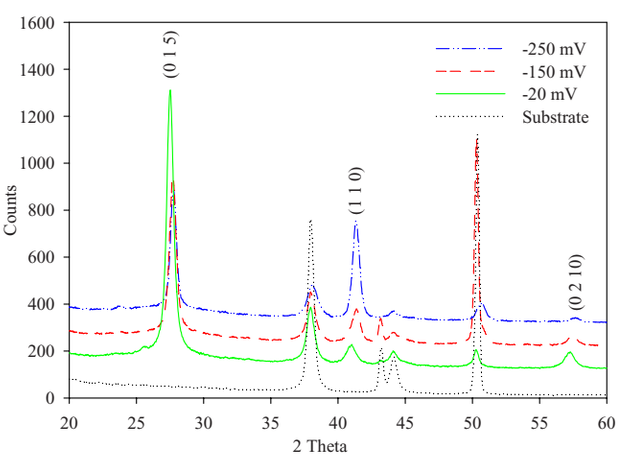

Figure 4. (Color online) XRD of the nanowires deposited in polycarbonate template.

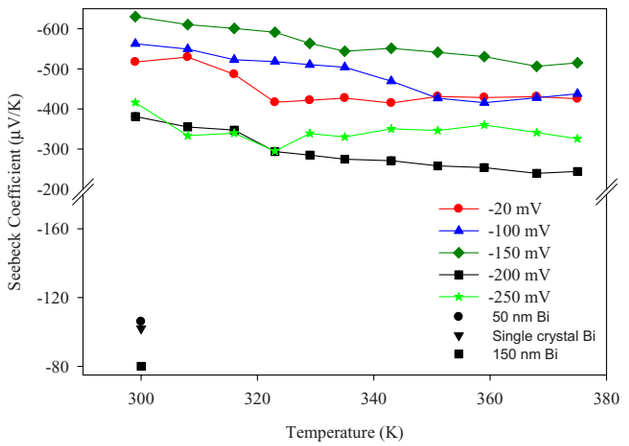

Figure 5. (Color online) Measurements of Seebeck coefficient of BiSbTe nanowires with respect to temperature. Reference Seebeck measurements for pure Bi nanowires of 50, 150,[14] and single crystal Bi[15] are also shown.

counterparts.[12] Increasing the Sb doping concentration (20–23%) induced the extrinsic holes that nullify the electrons contribution, resulting to an overall decrease in Seebeck coefficient for n-type materials.

Conclusions

We have electrodeposited BiSbTe nanowires into polycarbonate templates from a tartaric–nitric acid based electrolyte and identified optimum potentials to deposit BiSbTe alloy nanowires. Composition analysis showed that antimony concentration in the alloy increased with the deposition potentials. The Seebeck coefficients of all the nanowires decreased with temperature, and the highest value of -630 μV/K was measured at 300 K for the $Bi_2Sb_{0.6}Te_3$ nanowire sample deposited at -150 mV. To the best of our knowledge this is the highest Seebeck coefficient reported for BiTe alloy materials.

Acknowledgments

This work is funded by LSBR P-KSFI and NASA (2008)-DART-30.

Louisiana Tech University assisted in meeting the publication costs of this article.

References

1. H. J. Goldsmid, *Thermoelectric Refrigeration*, Plenum, New York (1964).
2. M. S. Dresselhaus, G. Chen, M. Y. Tang, R. Yang, H. Lee, D. Wang, Z. Ren, J. P. Fleurial, and P. Gogna, *Adv. Mater.*, **19**, 1043 (2007).
3. R. Venkatasubramanian, E. Siivola, T. Colpitts, and B. O'Quinnet, *Nature (London)*, **413**, 597 (2001).
4. M. S. Dresselhaus, Y. M. Lin, O. Rabin, A. Jorio, A. G. Souza Filho, M. A. Pimenta, R. Saito, G. G. Samsonidze, and G. Dresselhaus, *Mater. Sci. Eng., C*, **23**, 129 (2003).
5. A. Mavrokefalos, A. L. Moore, M. T. Pettes, L. Shi, W. Wang, and X. Li, *J. Appl. Phys.*, **105**, 104318 (2009).
6. M. Martín-Gonzalez, A. L. Prieto, R. Gronsky, T. Sands, and A. M. Stacy, *Adv. Mater.*, **15**, 1003 (2003).
7. D. Del Frari, S. Diliberto, N. Stein, C. Boulanger, and J.-M. Lecuire, *Thin Solid Films*, **483**, 44 (2005).
8. D. Del Frari, S. Diliberto, N. Stein, C. Boulanger, and J. M. Lecuire, *J. Appl. Electrochem.*, **36**, 449 (2006).
9. F. Xiao, B. Yoo, K. H. Lee, and N. V. Myung, *Nanotechnology*, **18**, 335203 (2007).
10. H. Bottner, G. Chen, and R. Venkatasubramanian, *MRS Bull.*, **31**, 211 (2006).
11. F. Xiao, C. Hangarter, B. Yoo, Y. Rheem, K. H. Lee, and N. V. Myung, *Electrochim. Acta*, **53**, 8103 (2008).
12. B. Lenoir, A. Dauscher, M. Cassart, Y. I. Ravich, and H. Scherrer, *J. Phys. Chem. Solids*, **59**, 129 (1998).
13. R. Mannam, M. Agarwal, A. Roy, V. Singh, K. Varahramyan, and D. Davis, *J. Electrochem. Soc.*, **156**, B871 (2009).
14. A. Nikolaeva, T. E. Huber, D. Gitsu, and L. Konopko, *Phys. Rev. B*, **77**, 035422 (2008).
15. C. F. Gallo, B. S. Chandrasekhar, and P. H. Sutter, *J. Appl. Phys.*, **34**, 144 (1963).
16. M. S. Martín-Gonzalez, A. L. Prieto, R. Gronsky, T. Sands, and A. M. Stacy, *J. Electrochem. Soc.*, **149**, C546 (2002).
17. O. Rabina, Y. M. Lin, and M. S. Dresselhaus, *Appl. Phys. Lett.*, **79**, 81 (2001).
18. B. Lenoir, M. Cassart, J. P. Michenaud, H. Scherrer, and S. Scherrer, *J. Phys. Chem. Solids*, **57**, 89 (1996).